Future dryness in the southwest US and the hydrology of the early 21st century drought

Daniel R. Cayan[a,b,1], Tapash Das[a], David W. Pierce[a], Tim P. Barnett[a], Mary Tyree[a], and Alexander Gershunov[a]

[a]Division of Climate, Atmospheric Sciences, and Physical Oceanography, Scripps Institution of Oceanography, La Jolla, CA 92093-0224; and [b]United States Geological Survey, La Jolla, CA 92093-0224

Edited by Glen M. MacDonald, University of California, Los Angeles, CA, and accepted by the Editorial Board March 18, 2010 (received for review October 26, 2009)

Recently the Southwest has experienced a spate of dryness, which presents a challenge to the sustainability of current water use by human and natural systems in the region. In the Colorado River Basin, the early 21st century drought has been the most extreme in over a century of Colorado River flows, and might occur in any given century with probability of only 60%. However, hydrological model runs from downscaled Intergovernmental Panel on Climate Change Fourth Assessment climate change simulations suggest that the region is likely to become drier and experience more severe droughts than this. In the latter half of the 21st century the models produced considerably greater drought activity, particularly in the Colorado River Basin, as judged from soil moisture anomalies and other hydrological measures. As in the historical record, most of the simulated extreme droughts build up and persist over many years. Durations of depleted soil moisture over the historical record ranged from 4 to 10 years, but in the 21st century simulations, some of the dry events persisted for 12 years or more. Summers during the observed early 21st century drought were remarkably warm, a feature also evident in many simulated droughts of the 21st century. These severe future droughts are aggravated by enhanced, globally warmed temperatures that reduce spring snowpack and late spring and summer soil moisture. As the climate continues to warm and soil moisture deficits accumulate beyond historical levels, the model simulations suggest that sustaining water supplies in parts of the Southwest will be a challenge.

climate change | regional modeling | sustainability | water resources

Persistent dry conditions have generally prevailed in the Southwest during the early years of the 21st century (1), after wetter than normal conditions in the preceding years. Such droughts have substantial impacts on the humans, animals, and plants inhabiting the Southwest, and call into question whether we can sustain the water resources that we have come to depend upon in the 20th century. This study uses high resolution ($1/8° \times 1/8°$) hydrological model simulations, driven by observed and downscaled global climate model meteorological fields, to investigate the region's droughts. Our goals are to place the 21st century drought into the context of the 20th century, and determine how Southwest drought is likely to change from its 20th century patterns in the future.

The Southwest's hydrology is marked by strong variability on seasonal to multiannual time scales, reflecting its sensitivity to fluctuations in large scale atmospheric circulation patterns. Preinstrumental paleoclimate records indicate that periods of extreme dryness have occurred sporadically during the last millennium (2, 3), so the 21st century drought is far from unprecedented. Some of the most prominent of these prehistoric droughts occurred in the midst of anomalously warm conditions, perhaps in similar fashion to the recent early 21st century drought. A protracted period of such dry conditions is likely to make currently scheduled water deliveries from the Colorado River unsustainable in the future, and have other significant impacts on the Southwest's inhabitants (4, 5).

Although the recent drought may have significant contributions from natural variability, it is notable that hydrological changes in the region over the last 50 years cannot be fully explained by natural variability, and instead show the signature of anthropogenic climate change (6–9). GCM projections show reduced precipitation over many lower midlatitude continental regions, including the Southwest, as the climate warms from greenhouse gases (10–13). The obvious question is whether the 21st century drought is the harbinger of things to come.

Besides having enormous economic and societal consequences, drought has considerable effects upon ecosystems. An epidemic of conifer tree die-offs in western US forests has been provoked by severe dryness and insect infestation, evidently exacerbated by warmer temperatures in both the growing and cool seasons (14–16). An increase in the number and areal extent of wildfire in middle elevation forests (17) has been attributed to an advance in spring snowmelt and warmer spring and summer temperatures. Likely warming and possible drying of the climate in future decades is projected to increase the occurrence and impact of wildfires over much of the Southwest (18). All these applications motivate a detailed examination of Southwest droughts.

Data and Models

We use observed temperature and precipitation to force the Variable Infiltration Capacity (VIC) hydrological model on a $1/8° \times 1/8°$ grid across the western US. This allows us to analyze VIC's estimates of key hydrological fields, such as soil moisture, that are poorly observed over the historical time period. VIC has been shown to produce realistic simulations of the hydroclimate's mean and variability in this region (8, 19, 20). We will refer to these estimates as VIC-OBS. *SI Text* (sections S1 and S2) contains details on the hydrological modeling process.

We use twelve global climate models (GCMs) used in the Intergovernmental Panel on Climate Change (IPCC) Fourth Assessment Report (10, 11) to investigate effects of climate change on the Southwestern United States. The full list of models is given in *SI Text* (section S3). We further analyze the output of two of the twelve models, Geophysical Fluid Dynamics Laboratory (GFDL) CM2.1 and Centre National de Recherches Météorologiques (CNRM) CM3. These two models produce temperature and precipitation simulations falling within the larger ensemble of changes from the set of 12 GCMs, and were among the few models that provided the continuous daily output necessary to drive VIC. More information on the simulation quality of these models is given in *SI Text* (section S3). We statistically downscale the

Author contributions: D.R.C. and T.P.B. designed research; D.R.C., T.D., D.W.P., M.T., and A.G. performed research; T.D., D.W.P., M.T., and A.G. analyzed data; and D.R.C., T.D., and D.W.P. wrote the paper.

The authors declare no conflict of interest.

This article is a PNAS Direct Submission. G.M.M. is a guest editor invited by the Editorial Board.

[1]To whom correspondence should be addressed. E-mail: dcayan@ucsd.edu.

This article contains supporting information online at www.pnas.org/lookup/suppl/doi:10.1073/pnas.0912391107/-/DCSupplemental.

GFDL CM2.1 and CNRM CM3 meteorological output fields to the same $1/8° \times 1/8°$ grid as the observations, using the method of constructed analogues (8, 21). We apply the models' downscaled meteorological fields to VIC to produce gridded estimates of soil moisture and runoff, which we term VIC-MOD. This method provides a consistent treatment between the models and observations when analyzing the hydrological fields.

Warming in the CNRM and GFDL simulations ranges from about 2– 4 °C by the latter half of the 21st century (Fig. S1*A*). Southwest precipitation changes little in the CNRM simulations, and declines in the GFDL simulations (Fig. S1*B*). These changes are representative of precipitation trends from the full set of IPCC models (10, 11), which show broad scale drying over lower midlatitude continental regions. The model simulation period used here is 1950–2100. We analyze in terms of water years, so, for example, "water year 2000" means October 1999 through September 2000. Projected 21st century hydrological conditions over the 21st century are evaluated with respect to historical and model simulated conditions within the 1951–1999 water year period. We used the IPCC Special Report on Emissions Scenarios (SRES) A2 and SRES B1 greenhouse gas emissions scenarios, representing medium high and moderately low emissions and associated global climate warming (10, 11).

We consider the Southwest to include the region from California to the eastern divide of the Rocky Mountains, and from the headwaters of the Colorado River in the central Rocky Mountains south to the Mexican border (Fig. 1). Although this region extends somewhat farther westward and northward than some traditional definitions of the Southwest, we included the California region together with the Great Basin and Colorado River basin because, to first order, the major arid portions of these three subregions have similar climate (22). They also have a moderate tendency for dry conditions to coincide (23; Table S1 and Fig. S2*A*). Finally, California and Nevada draw part of their water supply from the Colorado River, adding to the interdependency of resources across the three regions.

Results

Most Extreme Droughts, 1916–2008. We use VIC-OBS to identify extreme droughts: water years when the area-averaged soil moisture falls below the 10th percentile of the 1951–1999 historical period. There are 11 such years over 1916–2008, both in the Southwest as a whole and within each of the three subregions. Area-averaged soil moisture in VIC-OBS is calculated as the total amount of moisture in the soil at a point divided by the maximum capacity at that point, averaged over the region. We also tried total (nonnormalized) moisture in the soil over the region, and found the list of dry years little different. Individual subregions have their own list of extreme drought years—for example, California has the strongest dryness in the 1930s and Colorado in the 1950s (Table S2).

Three of the 11 extreme drought years we identified have occurred since the 21st century began: water years 2002, 2007, and 2008 (Table S2). The early 21st century drought started in water year 2000 with exceptionally warm temperatures across virtually the entire West, and precipitation in the 30th percentile or lower over most of the interior away from the Pacific coast. Even lower precipitation values were seen in the same general region in water year 2002, with a large swath from western Kansas through Colorado, Utah, Arizona, southern Nevada, and southern California receiving precipitation in the 20th percentile or below. Although temperatures peaked in water year 2000, they continued elevated almost every year through 2007, and were again warm in 2009. The last time water year averaged temperatures were >1 °C colder than usual across most of the western United States was in 1993, 16 years ago, although such cold years were experienced regularly before 1985.

For the Southwest as a whole, VIC-OBS estimated extreme drought years are clustered in the early 1930s, late 1950s and early 1960s, late 1980s and early 1990s, and in the late 2000s. The extreme dry years in the 20th century almost always have occurred in the midst of longer dry periods, in which droughts build up and subside over multiple years. The durations of these

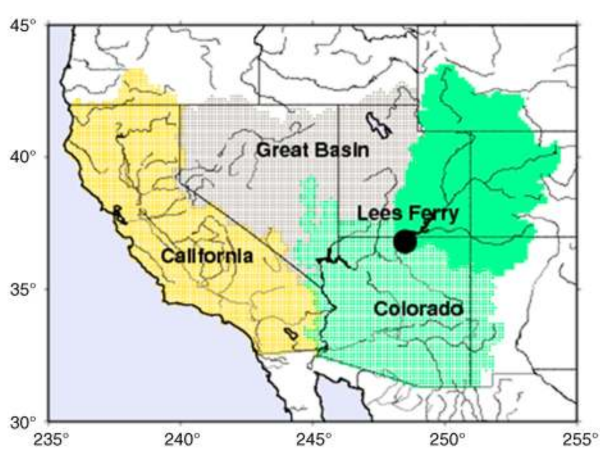

Fig. 1. The study area consists of three regions: California, Great Basin, and Colorado River Basin. Together these are called the "Southwest."

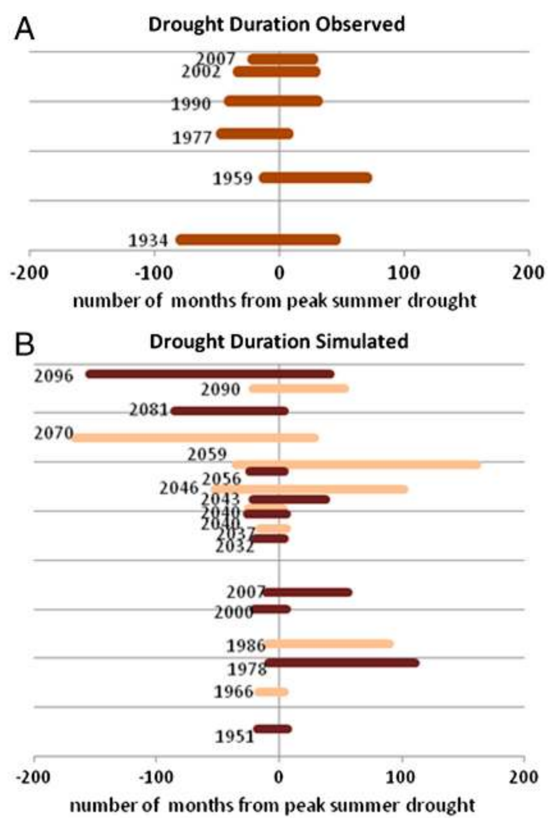

Fig. 2. Duration of dry intervals associated with extreme drought, as simulated by the VIC hydrological model. (*A*, *Upper*) From VIC forced by observed temperature and precipitation (VIC-OBS), 1915–2008. (*B*, *Lower*) From VIC forced by the CNRM (*Light*) and GFDL (*Dark*) global models under the SRES A2 emissions scenario (VIC-MOD). Years advance upward. In some cases these intervals include two or more of the extreme drought years. Period before/after each drought extreme was defined by the end /beginning of the first 6 month consecutive spell having unbroken negative soil moisture anomalies. In some cases these intervals include two or more of the extreme drought years. The duration of the 2007 dry spell is a minimum estimate because it was still not broken at the end of the dataset in December 2008.

prominent historical dry spells, based upon the time when Southwest-averaged soil moisture dropped and stayed below average for at least six months as an indicator of dry conditions, are shown in Fig. 2*A*. The duration of dryness surrounding the spell's peak summer drought has ranged from 47 to 123 months.

The dry spells projected over the 21st century through the lens of the CNRM and GFDL simulations, calculated using VIC-MOD, are shown in Fig. 2*B*. The incidence of extreme drought during the first half of the 21st century is little changed in either model or SRES scenario. But by the second half of the 21st century, the number and duration of extreme dry events increases markedly, with most of the projected dry spells lasting longer than 5 years and in three cases exceeding 150 months—more than 12 years.

Hydrological Characteristics of Southwest Droughts. Fig. 3 shows composite anomalies of selected hydrological measures for the 11 extreme dry years, using an extended sequence of 48 months. The sequence begins 2 years before the extreme dry year and continues through 1 year after. On average, annual runoff aggregated over the Southwest dropped to 63% of its historical norm during the peak drought year. The composite also shows that 2 years and 1 year prior to the peak dry year, annual runoff averaged 85% and 81% of the 1951–1999 water year average, whereas the year after the extreme drought year, composite runoff had only recovered to 80% of average.

The most recent dry spell, with extreme dryness in 2007, is evaluated below specifically for the Colorado River flow at Lees Ferry. It is also shown for the Southwest as a whole in Fig. 3 as the brown line. Over the larger region the episode does not have an unusual precipitation deficit, which is close to the average during 2006 and turns dry during the 2007 water year. Runoff, however, is below average extreme dry levels. Notably, the warmth of the recent drought is exceptionally strong and consistent, with a spell of positive temperature anomalies that is nearly unbroken from 2005 through the end of 2008.

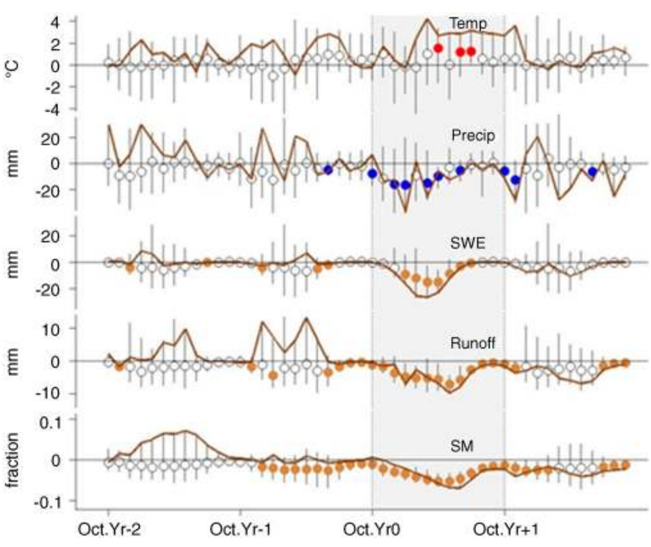

Fig. 3. Composite Southwest-area aggregated monthly anomaly of temperature, precipitation, snow water equivalent, runoff, and soil moisture beginning October, two years prior to the extreme drought year through September, and one year after the extreme drought year. Composites are average anomalies over the 11 historical drought cases. Composite anomalies (*Circles*) are calculated from 1951–1999 average monthly climatology, and those which are significant at the 95th percentile are colored. Vertical whiskers extend from the 5th percentile to the 95th percentile of the samples in the composite population. Anomalies that occurred before, during, and after the 2007 dry spell are shown by the solid brown line.

Fig. 3, a composite over the 11 extreme drought cases, shows that precipitation shortages often accumulate over many months in advance of the gravest drought conditions and persist over multiple years. Greatest precipitation shortfalls occur during the winter months when precipitation is normally at its maximum, but the composite shows that precipitation deficits may also occur during the fall and spring as the North Pacific storm season is transitioning from or to its summer inactive state. The below average precipitation gives rise to below average soil moisture; runoff responds directly to these conditions, with the composites showing largest reductions during the core drought year, but also negative anomalies during the prior buildup and subsequent persistence of low soil moisture conditions. Greatest soil moisture deficits occur in May and June, the period when soil moisture normally begins a rapid decline to low summer levels in the Southwest. Composited over the 11 extreme drought years, the aggregate Southwest precipitation was reduced to 77% of its 1951–1999 average, April 1 snow water equivalent was reduced to 50%, and runoff was reduced to 63%.

Drier Soils and Warmer Summer Temperatures. During drought events, warm summer temperature anomalies blanket the whole Southwest and spread over much of the conterminous United States (Fig. S2*B*). Monthly mean temperature anomalies in drought summers range from +0.5 °C to +1 °C (Fig. 3). Averaged over the water year during the extreme droughts, minimum temperatures (Tmin, usually nighttime) were 0.3 °C above average whereas maximum temperatures (Tmax, usually daytime) over the Southwest were 0.8 °C above the 1951–1999 average. The composite Tmin temperature anomaly approached 1 standard deviation whereas that for Tmax exceeded 1 standard deviation of the annual temperatures over the Southwest.

This linkage is also present with a strong degree of statistical confidence in the downscaled CNRM and GFDL simulations ($p < 0.05$), demonstrated when we stratify the years when VIC-MOD soil moisture or precipitation is below average vs. above average. It should be noted that CNRM was one of the models that registered the lowest degree of temperature change from wet to dry, although this model has demonstrated a strong degree of temperature response during dry continental high pressure regimes (24). The association of drier soils with warmer summer temperatures is found in most of the 12 GCM historical 20th century sequences and 21st century climate change simulations (Fig. S3).

Amplified Droughts Under Climate Warming. The Southwest becomes more arid over the 21st century in the CNRM and GFDL model simulations, as judged by changes in VIC-MOD's regional aggregate snow pack and soil moisture (Fig. 4 for CNRM only, and Fig. S4), with associated deficit precipitation and reductions in runoff.

The occurrence of years with April 1 snowpack low enough to qualify as being below the 10th percentile (based on the 1951–1999 historical period) changes little during the first half of the 21st century in VIC-MOD, but these very low snow years increase by 2.5–5 times during the last half of the 21st century, consistent with several previous regional climate change studies (25). Conversely, as climate warming advances, years with spring snowpack exceeding even the average historical value occur less and less often. Accompanying the loss of spring snowpack, years with extremely low early summer soil moisture occur more than twice as often during the second half of the 21st century (Fig. 4, *Lower Panel*).

The depletion of soil moisture during dry events in VIC-MOD is both prolonged and magnified during the second half of the 21st century (Fig. 2*B* and Fig. S4). Composites of soil moisture anomalies show progressive deficits in years both preceding and following peak drought years (Fig. S5). The number of extreme

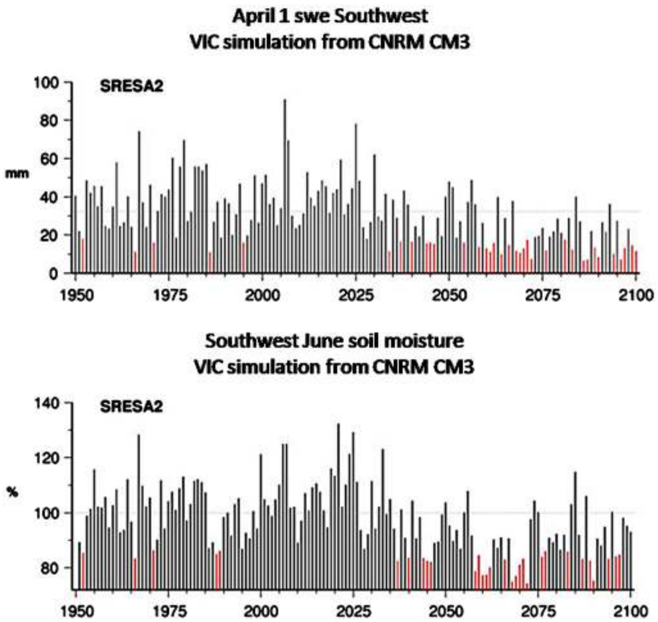

Fig. 4. Southwest region April first snow water equivalent (mm) (*Upper*) and June soil moisture (% of 1951–1999 average annual values) (*Lower*) from VIC simulation of the CNRM CM3 GCM for 1950 to 2100. Climate change period (2000–2100) from scenarios SRES A2. Extremely dry years are indicated by red bars that mark years when April 1 SWE or June soil moisture is lower than the 10th percentile of the historical (1951–1999) period (18.0 mm).

drought years in the two models, determined using the same criteria as for the observed cases, showed no change or actually decreased during the 2000–2049 period, but increased from 5 events during the climatological period to 6 and 9 (SRES B1) and 9 and 13 (SRES A2) during 2050–2099 (Table 1). During the extreme droughts, the relative deficit in soil moisture grows larger, and also grows in comparison to the deficit in precipitation, as judged by standardized precipitation and soil moisture anomalies shown in Fig. 5*A*. Over the historical period, the annual precipitation anomalies during drought are about 1.3 standard deviations below their climatological mean, whereas VIC-OBS and VIC-MOD soil moisture anomalies for extreme droughts are approximately 1.5 standard deviations below their climatological mean. But by end of 21st century, the soil moisture deficits range from 1.7 to more than 2 standard deviations below the mean. Because average precipitation anomalies during a drought do not change as much for the late 21st century, we conclude that more of the water budget is being consumed by other processes, probably evapotranspiration, which results in the amplified soil moisture deficit compared to precipitation deficit.

Table 1. Southwest drought year counts from simulations. A drought year is defined when southwest aggregate soil moisture falls below its historical 1951–1999 10th percentile value. Climate change period soil moisture from VIC hydrologic simulations forced by results from GCMs CNRM CM3 and GFDL CM2.1. Climate change simulations from two global greenhouse gas scenarios SRES A2 and SRES B1.

Counts of extreme droughts, climate simulations

		Historical *1951–1999*	Projected early period *2000–2049*	Projected late period *2050–2099*
CNRMCM3	SRESA2	5	3	9
	SRESB1	5	2	6
GFDLCM2.1	SRESA2	5	5	13
	SRESB1	5	4	9

Recent Drought in the Colorado Basin—Could it get Worse? The increasing duration and severity of drought conditions we have described could have a particularly deleterious effect on Colorado River water supplies. Because the water in the river is already completely allocated, this leads to questions of whether those allocations are sustainable. Is the early 21st century drought on the Colorado River unusual or can we expect others like it in the future?

Some droughts are short and intense whereas others are less deep but persistent. From the point of view of a reservoir system, it is the total deficit in flow over some period that matters. With this drought indicator in mind, we used a stochastic Colorado River flow model to estimate flow conditions at Lees Ferry over 2000 realizations of the last 100 or so years. The realizations were generated by Fourier transforming the observed flow, randomizing the phases, and transforming back; the result shows good agreement with both historically observed flow and paleoclimate estimates from tree rings (26). The various realizations were then used to estimate the probability of observed drought sequences over the last 100 + years. Were any of them "unusual?"

From the 2000 realizations, we calculated the accumulated deficit in flow over N years, taking N from 1 to 10. The deficit is calculated relative to what the total flow would have been if the simple mean flow over the historical period had gone down the river each year. For example, if the mean flow is 18×10^9 m^3/year (billion cubic meters per year, or bcm/year) and the 5-year running mean in year 1960 is 14 bcm/year, then the accumulated deficit in 1960 for $N = 5$ years is $5^*(18 - 14) = 20$ bcm.

Fig. 5*B* shows the accumulated deficit in Colorado River flow as a function of N for the historical period, 1906–2008. Each year is shown as a dot, plotted at the value of N that gives the largest accumulated deficit. The observed early 21st century drought is highlighted in red. Gray shading indicates the region that will contain the worst drought of the century 2/3 of the time, calculated from the 2000 realizations. There is a 1/3 chance of a drought worse than shown (i.e., falling below the shading), but essentially no chance ($p < 0.005$) of the worst-in-century drought being better. The early 21st century drought falls squarely in this region ($p \sim 0.6$). Other details on the figure are given in *SI Text* (section S4).

An alternative explanation for the occurrence of this severe drought in recent times could be the initial impacts of global warming described above. Indeed, most studies predict a reduction Colorado River flow as warming impacts intensify (see ref. 5 for a list). The effects of this warming have been detected in the hydrological cycle of the western United States (6–9). The green hatched region in Fig. 5*B* shows ensemble-averaged estimates from VIC-MOD of where the worst drought of the century will likely fall, using the SRES A2 scenario and model-projected flow from 2050–2099. The models suggest the early 21st century drought will become commonplace in the future, and that the worst drought of the century will be much more severe than we have experienced since measurements began.

The climate model simulations indicate that there may be substantial differences in the amount of drying across the broad Southwest region. These differences are confirmed when this analysis is repeated for flow in the Sacramento River above Bend Bridge, whose watershed lies in the northernmost California portion of our domain. First, flows are not unusually low in the early 2000s, unlike the Colorado River result (Fig. S6). Second, the climate change shift is toward wetter conditions, not drier. Thus it appears that only certain core areas, such as the Colorado basin, could experience harsher droughts.

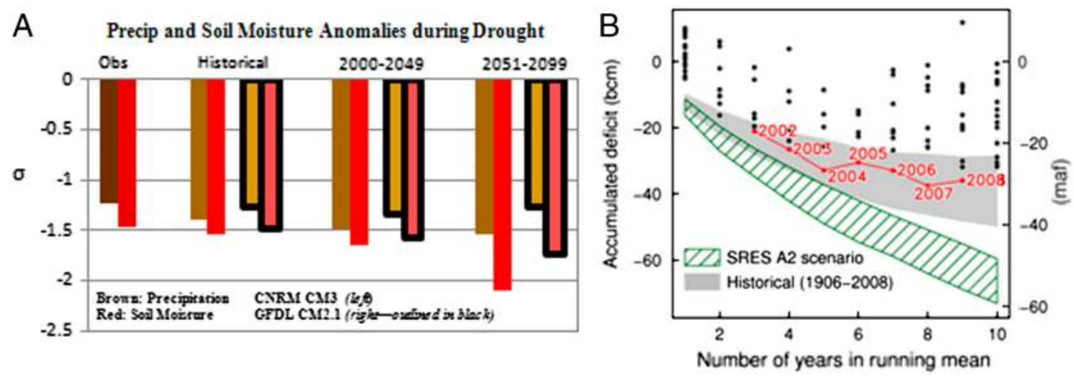

Fig. 5. (*A*, *Left*) Composite of water year precipitation and water year soil moisture (*Red*) anomalies associated with extreme negative soil moisture anomalies for Southwest from historical observation and simulated climate input from CNRM CM3 and GFDL CM2.1 GCMs SRES A2 emission scenario—historical period 1951–1999, early 21st century 2000–2049 period, and late 21st century 2050–2099 period. In the figure, precipitation and soil moisture composites are shown side by side. For climate model simulation, composites from CNRM CM3 are shown first, and then from GFDL CM2.1, for each time epoch. (*B*, *Right*) Accumulated deficit in flow [10**9 m**3, or billions of cubic meters(bcm)] on the Colorado River at Lees Ferry, relative to the mean flow observed over the period 1906–2008. Deficit is calculated in N-year running means (X axis). The 21st century drought is shown in red; other years are shown as black dots. Gray shading indicates where, 2/3 of the time, the worst drought of the century should fall; the green hatched region shows the same thing for the end of this century, estimated from downscaled climate models. The right hand axis additionally shows values in millions of acre-feet (maf). See text for details. (For Sacramento at Bend Bridge, see Fig. S6).

At this point, it is not possible to say which mechanism (chance or warming) is responsible for the observed dryness in the Colorado basin during the first years of the 21st century. But whichever it is, the clear message is that a drought equally severe is quite likely to reoccur during the rest of the 21st century.

Discussion

The early 21st century drought is an example of the kinds of droughts the Southwest United States is prone to. Such droughts have a tendency to take on large southwest footprints, although both observations and climate model simulations display different degrees of dryness in California, the Great Basin, and the Colorado basin. This is true for the early 21st century drought as well, which is more severe in the Colorado basin than in California. As quantified by the VIC hydrological model, the most extreme drought years throughout the instrumental record have tended to build up and finally abate over an extended multiyear period. Historically, and especially during the early 21st century, observed Southwest droughts have been exacerbated by anomalously warm summer temperatures. This tendency may continue—several different 21st century climate model simulations suggest that dry years will experience anomalously warm summer temperatures, even above and beyond the warming trend in the Southwest.

The recent drought in the Colorado basin has seen the lowest accumulated deficit in flows at Lees Ferry in over a century of measurements, and has only a 60% chance of occurring in a century. However, given the amount of natural variability in the region's runoff, the current drought is not outside the realm of droughts likely to be encountered due to natural variability. Downscaled climate model projections show longer and more intense future droughts in the Colorado basin, and a high likelihood of worst-in-century droughts with multiyear flow deficits that exceed any in the observational record by 60–70%. If these climate scenarios materialize, we will have to prepare for deeper and historically more unusual water shortages, and the sustainability of current water deliveries from the Colorado River will become problematical.

In summary, a view from a small, but representative selection of climate simulations downscaled to $1/8^{\circ} \times 1/8^{\circ}$ and applied to a hydrological model suggests a future where drought becomes more extreme by the mid to late 21st century. Inevitably, there will be precipitation shortages, and during these times, the resulting hydrological drought is aggravated by a trend toward much less snowpack, warmer temperatures (especially in summer) and diminished runoff and soil moisture.

ACKNOWLEDGMENTS. We thank Andrew W. Wood, Edwin P. Maurer, Alan F. Hamlet, Dennis Lettenmaier, and Francisco Munoz-Arriola, for the VIC model, forcing, and parameters. We thank two anonymous reviewers and editor for important comments. Naturalized streamflow data for the Colorado River at Lees Ferry was obtained from James Prairie of the Bureau of Reclamation. Part of the downscaled data was developed by Hugo Hidalgo. Jennifer Johns provided illustrations and expert processing of the manuscript. We acknowledge the several international global climate modeling groups, and particularly at Centre National de Recherches Météorologiques (CNRM) and Geophysical Fluid Dynamics Laboratory (GFDL) for global climate model output. We thank the Program for Climate Model Diagnosis and Intercomparison and the World Climate Research Program (WCRP) Working Group on Coupled Modeling for the WCRP Coupled Model Intercomparison Project phase 3 (CMIP3) multimodel dataset. Support of this dataset is provided by the Office of Science, US Department of Energy.

Funding was provided by the California Energy Commission Public Interest Energy Research Program through the California Climate Change Center, by the National Oceanic and Atmospheric Administration Regional Integrated Sciences and Assessments Program through the California Applications Program. The CALFED Bay-Delta Program postdoctoral fellowship provided partial salary support for T.D.

1. MacDonald GM, et al. (2008) Climate warming and 21st century drought in southwestern North America. *Eos Transactions, American Geophysical Union* 89(9):82–83.
2. Cook ER, Woodhouse C, Eakin CM, Meko DM, Stahle DW (2004) Long-term aridity changes in the western United States. *Science* 306:1015–1018.
3. Woodhouse CA, Meko DM, MacDonald GM, Stahle DW, Cook ER (2010) A 1,200-year perspective of 21st century drought in southwestern North America. *Proc Natl Acad Sci USA* 107:21283–21288.
4. Gober PA, Kirkwood CW (2010) Vulnerability assessment of climate-induced water shortage in Phoenix. *Proc Natl Acad Sci USA* 107:21295–21299.
5. Barnett TP, Pierce DW (2009) Sustainable water deliveries from the Colorado River in a changing climate. *Proc Natl Acad Sci USA* 106:7334–7338.
6. Barnett TP, et al. (2008) Human-induced changes in the hydrology of the western US. *Science* doi:10.1126/science.1152538.
7. Pierce DW, et al. (2008) Attribution of declining western US snowpack to human effects. *J Climate* 21:6425–6444.
8. Hidalgo HG, et al. (2009) Detection and attribution of streamflow timing changes to climate change in the western United States. *J Climate* 22:3838–3855.
9. Das T, et al. (2009) Structure and origins of trends in hydrological measures over the western United States. *J Hydrometeorol* 10:871–892 doi:10.1175/2009JHM1095.1.
10. Intergovernmental Panel on Climate Change Solomon S, et al., ed. (2007) *Climate Change 2007: The Physical Science Basis. Contribution of Working Group I to the Fourth Assessment Report of the Intergovernmental Panel on Climate Change* (Cambridge University Press, Cambridge, UK).
11. Intergovernmental Panel on Climate Change (2007) *Impacts, Adaptation, and Vulnerability: Contribution of Working Group II to the Intergovernmental Panel on Climate Change Fourth Assessment Report.*

12. Seager R, et al. (2007) Model projections of an imminent transition to a more arid climate in southwestern North America. *Science* 316:1181–1184.
13. Cook ER, et al. (2010) Megadroughts in North America: Placing IPCC projections of hydroclimatic change in a long-term palaeoclimate context. *J Quaternary Sci* 25:48–61.
14. Allen CD (2007) Cross-scale interactions among forest dieback, fire, and erosion in northern New Mexico landscapes. *Ecosystems* 10:797–808.
15. Yuhas AN, Scuderi LA (2009) MODIS-derived NDVI characterisation of drought-induced evergreen dieoff in western North America. *Geogr Res* 47:34–45 doi:10.1111/j.1745-5871.2008.00557.
16. Williams AP, et al. (2010) Forest responses to increasing aridity and warmth in the southwestern United States. *Proc Natl Acad Sci USA* 107:21289–21294.
17. Westerling AL, Hidalgo HG, Cayan DR, Swetnam TW (2006) Warming and earlier spring increase western US forest wildfire activity. *Science* 313:940–943.
18. Westerling AL, Bryant BP (2008) Climate change and wildfire in california. *Climatic Change* 87:231–249 doi: 10.1007/s10584-007-9363-z.
19. Liang X, Lettenmaier DP, Wood EF, Burges SJ (1994) A simple hydrologically based model of land surface water and energy fluxes for GSMs. *J Geophys Res* 99(D7): 14 415–14 428.
20. Maurer EP, Wood AW, Adam JC, Lettenmaier DP, Nijssen B (2002) A long-term hydrologically based dataset of land surface fluxes and states for the conterminous United States. *J Clim* 15:3237–3251.
21. Maurer EP, Hidalgo HG (2008) Utility of daily vs. monthly large-scale climate data: An intercomparison of two statistical downscaling methods. *Hydrol Earth Syst Sc* 12:551–563.
22. Diaz HF (2003) Biomes, river basins, and climate regions: Rational tools for water resource management. *Climate and Water: Transboundary Challenges in the Americas*, eds HF Diaz and BJ Morehouse (Kluwer, Boston), pp 221–235.
23. Cayan DR, et al. (2003) The transboundary setting of California's water and hydropower systems—Linkages between the Sierra Nevada, Columbia River, and Colorado River hydroclimates: Chapter 11. *Climate and Water—Transboundary challenges in the Americas*, eds HF Diaz and B Woodhouse (Kluwer, Boston), 16, pp 237–262.
24. Gershunov A, Douville H (2008) Extensive summer hot and cold extremes under current and possible future climatic conditions: Europe and North America. *Climate Extremes and Society*, eds H Diaz and R Murnane (Cambridge University Press, Cambridge, UK).
25. Christensen NS, Wood AW, Voisin N, Lettenmaier DP, Palmer RN (2004) Effects of climate change on the hydrology and water resources of the Colorado River basin. *Climatic Change* 62:337–363.
26. Barnett TP, Pierce DW (2008) When will Lake Mead go dry? *Water Resour Res* 44:W03201 doi:10.1029/2007WR006704.

Supporting Information

Cayan et al. 10.1073/pnas.0912391107

SI Text

SI Data and Models.

S1. Observational Data. Daily gridded meteorological observations of precipitation (P), maximum temperature (Tmax), minimum temperature (Tmin), and wind speed at 1/8 degree spatial resolution across the Southwestern Unites States were obtained from the Surface Water Modeling Group at the University of Washington (http://www.hydro.washington.edu; 1). The data are based on the National Weather Service cooperative network of weather observations stations, augmented by information from the higher quality Global Historical Climatology Network (GHCN) stations.

The dataset in ref. 1 is available for the period 1915 through 2003. To extend the dataset up to 2008, we used daily gridded meteorological fields for the period 2004 through 2008 produced by the same group (the Surface Water Modeling Group at the University of Washington) based on a reduced set of stations. This reduced set is available with near-real-time updates, because it is used operationally for a West-wide seasonal hydrologic forecast system (2).

S2. The Variable Infiltration Capacity (VIC) hydrologic model. To produce hydrologic variables during the 20th century and under 21st century climate change conditions, we used the VIC distributed macroscale hydrologic model (3). Defining characteristics of VIC are the probabilistic treatment of subgrid soil moisture capacity distribution, the parameterization of baseflow as a nonlinear recession from the lower soil layer, and the unsaturated hydraulic conductivity at each particular time step is treated as a function of the degree of soil saturation (3, 4). It uses a tiled representation of the land surface within each model grid cell, allowing subgrid variability in topography, infiltration, and land surface vegetation classes (3, 4).

The VIC model was run at a daily time step, with a 1-hour snow model time step in water balance mode, and using a 1/8 by 1/8 degree resolution grid across the Southwestern United States. Using the gridded observed meteorological forcing (described below), along with the physiographic characteristics of the catchment (for example, soil and vegetation), VIC calculates a suite of hydrologic variables, including runoff, baseflow, soil moisture, actual evapotranspiration and snow water equivalent in the snowpack. Derived variables such as radiation, humidity, and pressure are estimated internally based on the input P, Tmax, and Tmin (5, 6).

VIC has been used extensively in a variety of water resources applications; from studies of climate variability, forecasting and climate change studies (2, 4, 7–12). The model's soil moisture estimations produce reasonable agreement with the few point measurements available (4), and VIC-simulated streamflow validates well with observations when the model has been calibrated using streamflow data (4, 12).

VIC was forced using the observed gridded meteorology described above (1, 2), and with downscaled global climate model (GCM) data from 1950 to 2099 using two climate models: the Centre National de Recherches Météorologiques (CNRM) CM3 model, and the Geophysical Fluid Dynamics Laboratory (GFDL) CM2.1 model. We used both the SRES A2 and B1 emissions scenarios in this work. Daily precipitation (P) and maximum and minimum temperatures (Tmax, Tmin) from models were downscaled to 1/8 degree resolution using the constructed analogues (CA) statistical downscaling method (12, 13). For the future simulations, climatological wind speed (computed from the daily wind speed in ref. 4 for the period 1950–1999) was used. The downscaled climate fields are obtained by constructing linear combinations of previously observed weather patterns, including adjustments for model biases and loss of variance. Results using CA and those obtained with bias correction and spatial downscaling (BCSD), another statistical downscaling methodology, are qualitatively similar (13). An advantage of the CA method over the BCSD method is that CA can capture changes in the diurnal cycle of temperatures; the downside is that this requires daily data rather than monthly.

Our soil moisture indices were calculated as follows: (*I*) At each model time step, we combined the instantaneous moistures from VIC's three soil layers. (*ii*) At each point, we computed the maximum soil moisture possible at each point by combining the maximum soil moisture possible in each of the three soil layers. (The maximum soil moisture for each soil layer is equal to soil layer depth multiplied by its respective porosity.) (*iii*) At each model time step, the soil moisture fraction is equal to ratio of instantaneous moisture to the maximum possible moisture. Soil moisture was averaged across Southwest region. In the Southwest, the soil accumulates water from the beginning of the year until April, whereupon it dries until October.

S3. GCM Simulations. For the present study we selected simulations from 12 GCMs from the World Climate Research Program (WCRP) Coupled Model Intercomparison Project phase 3 (CMIP3) multimodel dataset: CNRM CM3, GFDL CM2.1, Center for Climate System Research (University of Tokyo) Model for Interdisciplinary Research On Climate (MIROC) 3.2 (medium resolution), European Center-Hamburg/Max Planck Institute ECHAM5/MPI OM, National Center for Atmospheric Research (NCAR) Community Climate System Model version 3 (CCSM3), NCAR Parallel Climate Model (PCM), Goddard space flight center Coupled General Circulation Model (CGCM) 3.1 (T47), Australian Commonwealth Scientific and Research Organization (CSIRO) Mk 3.0, Institut Pierre Simon Laplace (IPSL) CM4, United Kingdom Meteorological Office (UKMO) HadCM3, and UKMO HadGEM1. Documentation on the models can be found at http://www-pcmdi.llnl.gov/ipcc/model_documentation/pcc_model_documentation.php. These models were selected because they have been evaluated and used in previous investigations of climate change over the region (e.g., 14), so the results herein can be more easily compared to previously published results.

We selected CNRM CM3 and GFDL CM2.1 for detailed analysis because they provided the contiguous daily output of Tmin and Tmax necessary for the VIC hydrological model, and because their simulations lie within the range of temperature and precipitation projections produced by a set of several global climate model simulations of future climate over the Southwest (Fig. S1).

The performance of these two models in terms of their mean climate and variability of temperature and precipitation on seasonal, pentadal, and decadal timescales has been previously evaluated over the western United States (14). Also included in the evaluation was the models' ability to represent El Niño-Southern Oscillation (ENSO), the Pacific Decadal Oscillation (PDO), and the teconnected responses of temperature and precipitation to ENSO and PDO in our region of interest. Over the 42 metrics used, GFDL 2.1 was in the top third of models, whereas CNRM was in the bottom third. CNRM's performance was hampered by significant biases; however, it is worth pointing out that the downscaling we used removes these biases. In other aspects of its simulation, CNRM was nearer to the middle of the pack of the CMIP3 models.

Both models have an overly strong ENSO signal that extends too far to the west in the tropical Pacific, a common failing of the current generation of global climate models. CNRM also has an ENSO period that is closer to 3 years, while in nature it is more irregular and spreads toward longer timescales. GFDL 2.1 has a good simulation of ENSO's spectrum. Both models have a PDO that is overly trapped to the Kuroshio region off the coast of Japan, rather than having the maximum in the center of the North Pacific. The amplitude of CNRM's PDO is realistic, but GFDL's is too weak along the west coast of North America. GFDL 2.1 again has a spectrum of the PDO that is indistinguishable from observations given the considerable sampling uncertainties involved, while CNRM has an overly pronounced 10-year peak in the spectrum. These model limitations should be kept in mind when evaluating the downscaled results shown here.

We used simulations driven by two greenhouse gas emissions scenarios. The A2 emissions scenario represents a differentiated world in which economic growth is uneven and the income gap remains large between now-industrialized and developing parts of the world; people, ideas, and capital are less mobile so that technology diffuses more slowly. The B1 emissions scenario presents a future with a high level of environmental and social consciousness combined with a globally coherent approach to a more sustainable development. The A2 scenario has higher emissions than the B1 scenario.

S4. Constructing Fig. 5*B*. The observations used to construct Fig. 5*B* in the main text are taken from US Bureau of Reclamation estimates of naturalized flow of the Colorado River at Lees Ferry, updated as of September 16, 2009. Flow values should be considered provisional, especially for the most recent years.

Comparing model-estimated flows to observed flows requires dealing with model biases. Model flows were adjusted to have the same mean and standard deviation as observed over the period 1950–1999. Values for mean and standard deviation are: observations, (14.68,4.64) million acre-feet (maf); for the GFDL model, (17.65,6.18) maf; for CNRM, (16.30,3.99) maf.

Each year in the historical period, 1906–2008, is shown on Fig. 5*B* as a black or red dot. Each year will have an accumulated deficit for every value of the running mean window width N from 1 to 10 (shown on the X axis of the figure). However, the dot is only plotted at the X value that has the maximum accumulated deficit. For example, consider the N-year running mean ending in 1950. Perhaps the 1 year running mean deficit is -2, and the two year running mean deficit is $+3$, and the three year mean deficit is -7, etc., so that all the running mean deficits are $(-2,+3,-7,-5,1,4,0,-2,-1,1)$. In this case a dot would be plotted at $X=3$, because the three year running mean is the one with the greatest flow deficit. There are different numbers of dots in each vertical column partly by chance, and partly reflecting the typical length of droughts in the region.

1. Hamlet AF, Lettenmaier DP (2005) Production of temporally consistent gridded precipitation and temperature fields for the continental US. *J Hydrometeorol* 6:330–336.
2. Wood AW, Lettenmaier DP (2006) A testbed for new seasonal hydrologic forecasting approaches in the western US. *B Am Meteorol Soc* 87(12):1699–1712.
3. Liang X, Lettenmaier DP, Wood EF, Burges SJ (1994) A simple hydrologically based model of land surface water and energy fluxes for GSMs, *J Geophys Res* 99(D7):14415–14428.
4. Maurer EP, Wood AW, Adam JC, Lettenmaier DP, Nijssen B (2002) A long-term hydrologically based dataset of land surface fluxes and states for the conterminous United States. *J Climate* 15:3237–3251.
5. Kimball JS, Running SW, Nemani R (1997) An improved method for estimating surface humidity from daily minimum temperature. *Agricultural and Forest Meteorol*. 85:87–98.
6. Thornton PE, Running SW (1999) An improved algorithm for estimating incident daily solar radiation from measurements of temperature, humidity, and precipitation. *Agric. For. Meteorol.* 93:211–228.
7. Nijssen B, O'Donnell GM, Lettenmaier DP, Lohmann D, Wood EF (2001) Predicting the discharge of global rivers. *J Climate* 14:3307–3323.
8. Sheffield J, Wood EF (2007) Characteristics of global and regional drought, 1950–2000: Analysis of soil moisture data from off-line simulation of the terrestrial hydrologic cycle. *J Geophys Res* 112(D17115) doi:10.1029/2006JD008288.
9. Barnett TP, et al. (2008) Human-induced changes in the hydrology of the western US. *Science* doi:10.1126/science.1152538.
10. Wood AW, Leung LR, Sridhar V, Lettenmaier DP (2004) Hydrologic implications of dynamical and statistical approaches to downscaling climate model outputs. *Climatic Change* 62:189–216.
11. Das T, et al. (2009) Structure and origins of trends in hydrological measures over the western United States. *J Hydrometeorol* 10:871–892.
12. Hidalgo HG, et al. (2009) Detection and attribution of streamflow timing changes to climate change in the western United States. *J Climate* 22:3838–3855.
13. Maurer EP, Hidalgo HG (2008) Utility of daily vs. monthly large-scale climate data: an intercomparison of two statistical downscaling methods. *Hydrol Earth Syst Sc* 12:551–563.
14. Pierce DW, Barnett TP, Santer BD, Gleckler PJ (2009) Selecting global climate models for regional climate change studies. *Proc Natl Acad Sci* doi:10.1073/pnas.0900094106.

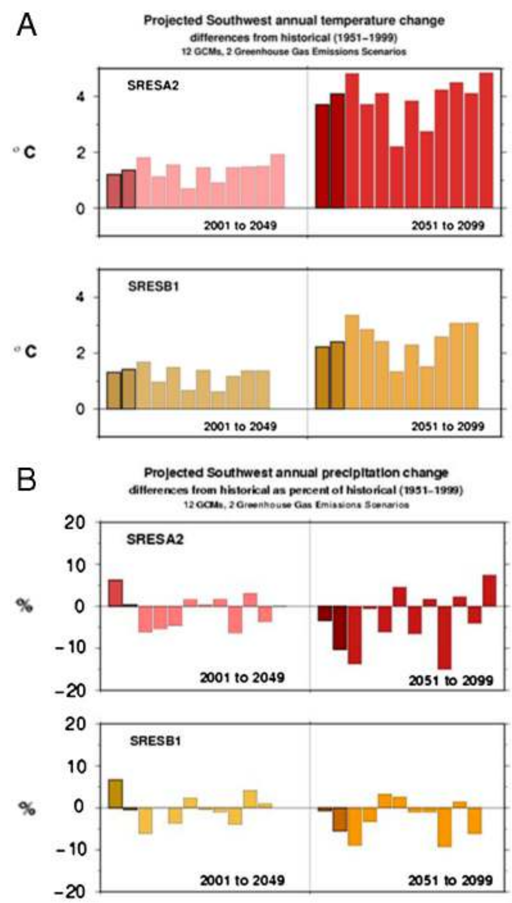

Fig. S1. Projected changes in annual temperature (*A*, *Upper*, °C) and precipitation (*B*, *Lower*, %) from the 12 CGMs used in this study. The 2 models analyzed in further detail (CNRM CM3 and GFDL CM2.1) are shown as outlined bars at the left of each row. Changes are relative to each model's historical period (1951–1999).

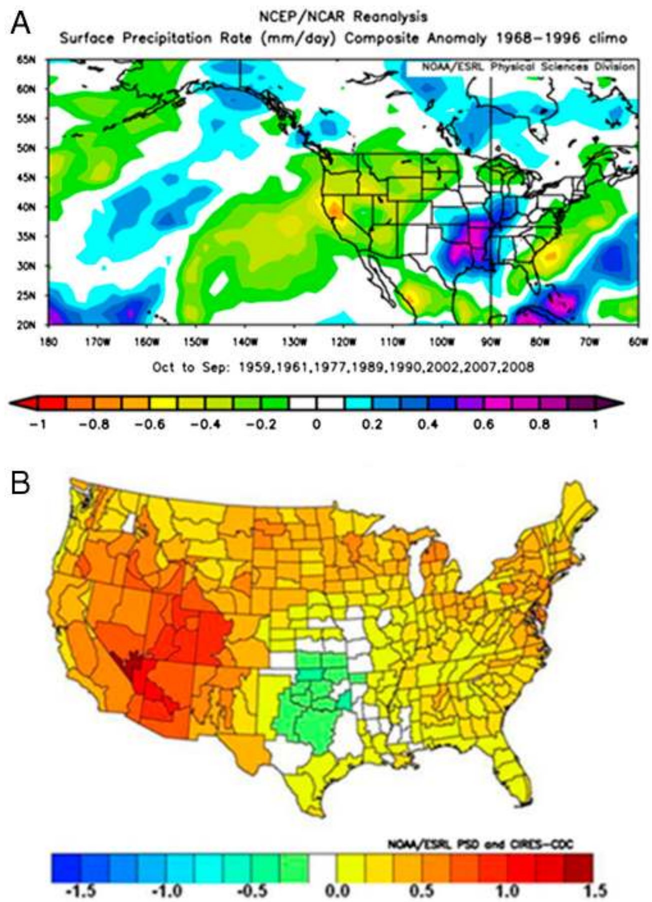

Fig. S2. (*A*, *Upper*) Composite precipitation rate (mm/day) over the water years of the extreme dry soil moisture years from National Center for Environmental Protection/National Center for Atmospheric Research (NCEP/NCAR) Reanalysis. Water years included are 1959, 1961, 1977, 1989, 1990, 2002, 2007, and 2008 (note that the reanalysis data starts in 1950). Water Year defined such that Water Year 2008 is October 2007–September 2008.). (*B*, *Lower*) Composite warm season (April–September) temperature anomalies (°C) during 11 extreme dry soil moisture years. These images are provided by the National Oceanic and Atmospheric Administration/Earth System Research Laboratory (NOAA/ESRL) Physical Sciences Division, Boulder Colorado from their Web site at http://www.psd.noaa.gov/ and use National Climatic Data Center (NCDC), 1994, Time Bias Corrected Divisional Temperature-Precipitation-Drought Index (TD-9640). Documentation for dataset TD-9640 is available from DBMB, NCDC, National Oceanic and Atmostpheric Administration.

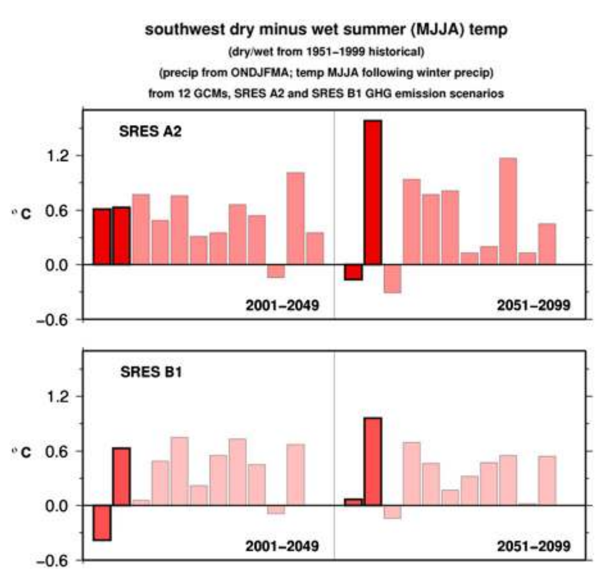

Fig. S3. Difference in May through August mean temperature: During years whose prior October through April precipitation is below average minus temperature for years whose prior October through April precipitation is above average. Scenario IPCC Special Report on Emissions Scenarios (SRES) A2 (*Upper*) and SRES B1 (*Lower*) for 2001–2049 and for 2051–2099.

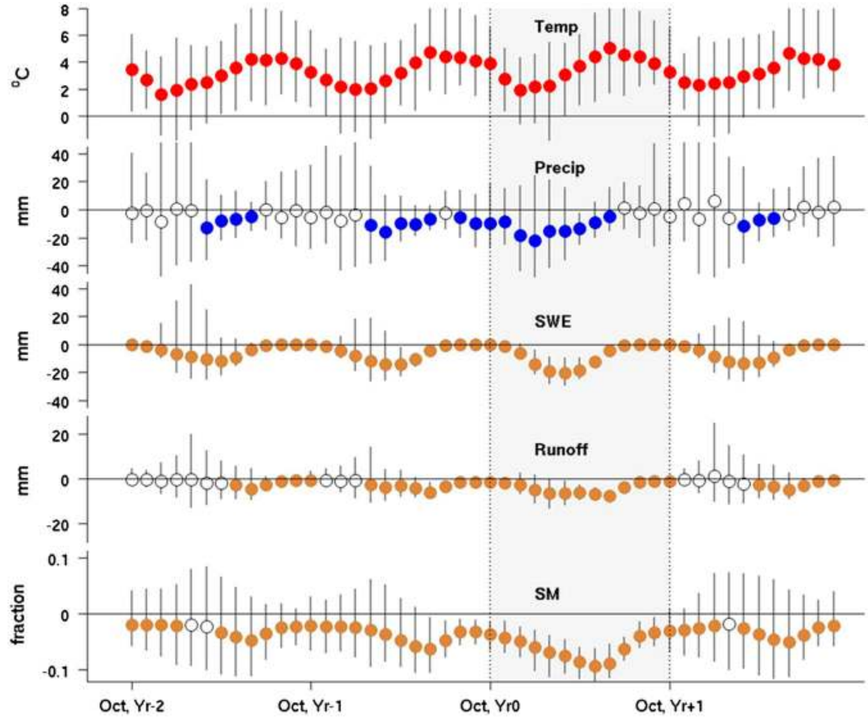

Fig. S4. Composite Southwest-area aggregated monthly anomaly of precipitation, snow water equivalent, runoff, and soil moisture beginning October, two years prior to the extreme drought year through September, one year after the extreme drought year. Composites are average anomalies over the drought cases identified from VIC simulations of CNRM CM3 and GFDL CM2.1 GCMs SRES A2 and SRES B1 emission scenarios, for the late 21st century 2050–2099 period. Composite anomalies (*Circles*) are calculated from 1951–1999 average monthly climatology, and those which are significant at the 95th percentile are colored. Vertical whiskers extend from the 5th percentile to the 95th percentile of the composite samples.

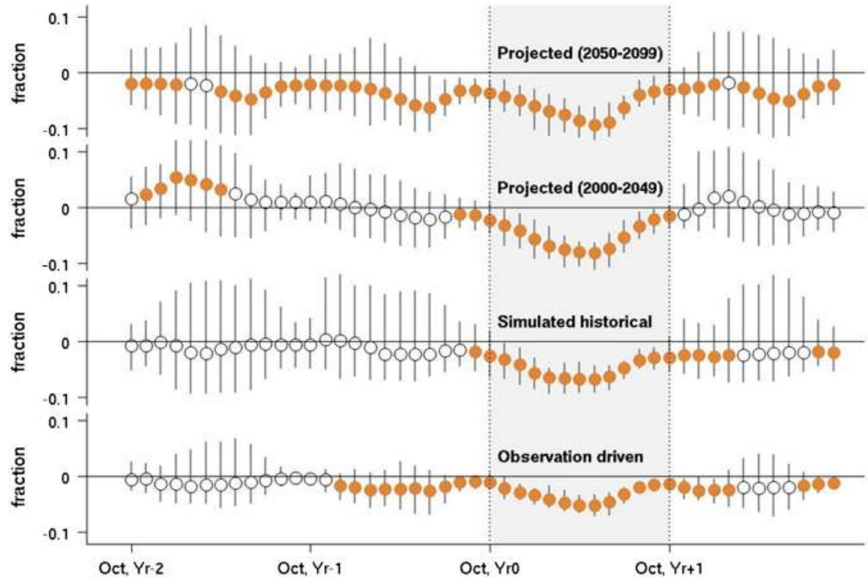

Fig. S5. Soil moisture anomalies composited on dry spells, for the historical period (1951–1999, *Lower Two Panels*), first half of the century, and second half of the century (*Upper Panel*). Values are from VIC driven by observations (*Lower*), and VIC driven by the downscaled CNRM CM3 and GFDL CM2.1 global models (*Other Panels*). Composite anomalies (*Circles*) are calculated from 1951–1999 average monthly climatology, and those which are significant at the 95th percentile are colored. Vertical whiskers extend from the 5th percentile to the 95th percentile of the composite samples.

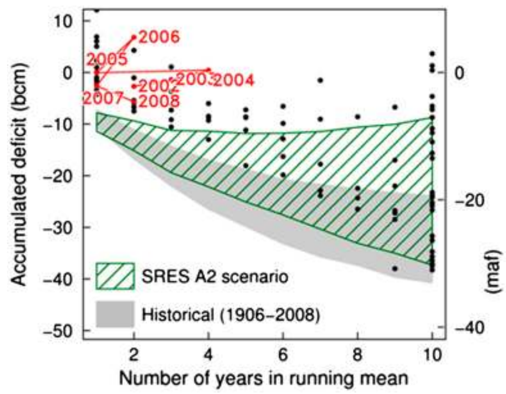

Fig. S6. As Fig. 4*B* in the main text, but calculated for the Sacramento River at Bend Bridge (south of Redding, California).

Table S1. Correlation among annual soil moisture (fraction of saturation) for different regions, in historical and climate change simulations

Correlation of Soil Moisture among Different Regions				
1916–1962 (from observed historical VIC simulations)				
	Southwest	*Colorado*	*Great Basin*	*California*
Southwest	1.00	0.76	0.75	0.75
Colorado	0.76	1.00	0.34	0.19
Great Basin	0.75	0.34	1.00	0.59
California	0.75	0.19	0.59	1.00
1963–2008 (from observed historical VIC simulations)				
	Southwest	*Colorado*	*Great Basin*	*California*
Southwest	1.00	0.87	0.94	0.86
Colorado	0.87	1.00	0.74	0.52
Great Basin	0.94	0.74	1.00	0.83
California	0.86	0.52	0.83	1.00
2000–2049 (median of four climate change simulations)				
	Southwest	*Colorado*	*Great Basin*	*California*
Southwest	1.00	0.85	0.90	0.88
Colorado	0.85	1.00	0.61	0.54
Great Basin	0.90	0.61	1.00	0.88
California	0.88	0.54	0.88	1.00
2050–2099 (median of four climate change simulations)				
	Southwest	*Colorado*	*Great Basin*	*California*
Southwest	1.00	0.87	0.92	0.90
Colorado	0.87	1.00	0.67	0.55
Great Basin	0.92	0.67	1.00	0.90
California	0.89	0.55	0.90	1.00

Soil moisture was simulated using VIC as driven by historical observed meteorology and downscaled meteorology from CNRM CM3 and GFDL CM2.1 GCMs, SRES A2 and SRES B1 emissions scenarios. For the climate change period, the median of the four climate change simulations are shown.

Table S2. Historical drought years

Historical Drought Years

	Southwest precip (mm)	Southwest soil moisture (fraction)	Southwest runoff (mm)		Great Basin precip (mm)	Great Basin soil moisture (fraction)	Great Basin runoff (mm)
1934	301	0.32	71	*1934*	210	0.38	15
2002	296	0.32	91	*1933*	224	0.38	23
1977	297	0.33	55	*1918*	276	0.39	27
1990	340	0.33	71	*1931*	225	0.39	17
1933	324	0.33	82	*1960*	228	0.39	23
2007	304	0.33	73	*2002*	229	0.39	26
1931	319	0.33	65	*1989*	264	0.40	26
1989	338	0.34	87	*2007*	226	0.40	13
1959	332	0.34	84	*1930*	283	0.40	29
2008	310	0.34	79	*1929*	292	0.40	31
1961	372	0.34	87	*1959*	260	0.40	22
Long Term Mean (1951–1999)	419	0.36	121	*Long Term Mean (1951–1999)*	320	0.43	44
	California precip (mm)	**California** soil moisture (fraction)	**California** runoff (mm)		**Colorado** precip (mm)	**Colorado** soil moisture (fraction)	**Colorado** runoff (mm)
1977	334	0.24	128	*2002*	217	0.31	25
1931	388	0.25	155	*1956*	248	0.32	35
1991	428	0.25	170	*1934*	265	0.33	25
1990	418	0.25	176	*1951*	302	0.33	37
1924	321	0.25	146	*1990*	334	0.33	32
2007	392	0.26	197	*1957*	366	0.33	48
1934	437	0.26	191	*1977*	287	0.34	27
2008	425	0.26	210	*1954*	327	0.34	32
1933	452	0.26	207	*1959*	293	0.34	31
1920	429	0.27	177	*1955*	303	0.34	32
1989	493	0.27	222	*1974*	275	0.34	39
Long Term Mean (1951–1999)	596	0.31	301	*Long Term Mean (1951–1999)*	359	0.36	48

A drought year is defined as a water year when the basin or regional aggregate, whole column soil moisture, averaged over the water year, falls below the 1951–1999 10th percentile value. Soil moisture was simulated using VIC as driven by historical observed meteorology. Using this criterion, a separate set of drought years is determined for the Southwest, Great Basin, California, and Colorado regions.